Evaluation of design methodologies for flexural strengthening of reinforced concrete structures with CFRP systems

Mariana Gato Canário Instituto Superior Técnico

Abstract

With the increasing number of rehabilitation and strengthening interventions on reinforced concrete (RC) structures, there has been a need to develop adequate repair/strengthening techniques, such as external bonding of fibre reinforced polymer composites (FRP), namely those with epoxy matrix in which carbon fibres are embedded (CFRP). The increasing use of this strengthening technique was complemented by the development of scientific studies, allowing for a better understanding of its mechanical performance and for the development of design guidelines; several documents about the topic are available nowadays.

The main goal of this dissertation is to analyse and compare the current design recommendations for flexural strengthening of RC structures using CFRP systems, either applied using the externally bonded technique (EBR) or the near surface mounted reinforcement (NSM) technique. This study starts with a presentation of the methodologies recommended in the current documents for the design of RC structures flexurally strengthened with CFRP systems; then, the different design methodologies are applied to practical design examples; finally, the predictions of the failure load obtained according to the different methodologies are compared to those obtained in flexural tests of RC beams and slabs strengthened with CFRP systems, available in the literature.

Based on the results obtained in the present study it was possible to conclude that the values determined according to by the main documents for the design strain of CFRP systems are, in general, conservative when compared to the experimental ones, especially those obtained with the methodology proposed in the annex of Eurocode 2.

1. Introduction

The use of CFRP materials to strengthen reinforced concrete (RC) structures has seen a considerable increase in the last decades, mainly due to the advantages they have when compared to traditional materials, namely steel. These benefits include their high strength, low weight, easy transportation and application and its high corrosion resistance. However, even with the previously mentioned benefits, the use of CFRPs has a relatively high initial cost, they present a linear elastic (i.e., brittle) behaviour and relatively frequent premature failure modes of the strengthening system occur at concrete-CFRP bond, preventing the high resistance capacity of the CFRP to be fully exploited. Over the last few years, the mechanical behaviour of reinforced concrete elements strengthened with CFRPs was an object of in depth and comprehensive studies; as a consequence, various international guidelines and codes for the design of RC structures flexurally strengthened with CFRP systems exist. However, in Portugal there are no standards/codes about this subject. Therefore, the design of a strengthening solution using CFRPs can result in very different areas, depending on which codes or guideline is adopted by the design engineer. The main goal of this dissertation consists in analysing the different recommendations for the design of RC structures strengthened with CFRP systems, either installed according with the externally bonded reinforcement (EBR) technique or the near surface mounted (NSM) technique. The main common and divergent points between the design philosophies for the CFRP strengthening systems adopted in the following documents will be pointed out: *fib* Bulletin 14 (2001) [1]; *fib* Bulletin 90 (2019) [2]; ACI-440.2R-17 the American Concrete Institute (2017) [3]; CNR-DT 200 R1/2012: Guide for the Design and Construction of Externally Bonded FRP Systems for Strengthening Existing Structures (2014) [4]; Annex J of EC2 – part 1 (2020) [5].

2. Design values for the CFRP strain

In order to define criteria for the design and safety verifications of flexural strengthening using CFRP systems, applied according the EBR or NSM techniques, it is necessary to identify and analyse their failure modes; the literature review demonstrated that failure modes involving CFRP debonding, are the most common ones. Figure 1 and figure 2 present these failure modes for EBR and NSM techniques, respectively. Regarding the design methods suggested in the various documents to obtain the flexural strength capacity in the most stressed (i.e., critical) sections, these are similar to each other and the most restraining factors are the different recommendations given in the documents for the design strain of the CFRP. In the next section, in order to highlight these differences, the recommendations given in the different documents (cf. table 1) will be applied to practical design examples and then compared to the experimental results available in the literature for both EBR and NSM techniques.

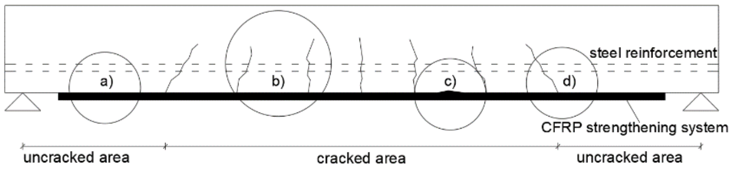

Caption:
- **mode a)**: CFRP end debonding;
- **mode b)**: Intermediate debonding caused by flexural cracks;
- **mode c)**: debonding caused by irregularities and roughness of concrete surface;
- **mode d)**: debonding caused by diagonal shear cracks.

Figure 1 – Failure modes by debonding of the reinforced concrete element for EBR technique (adapted of [1]).

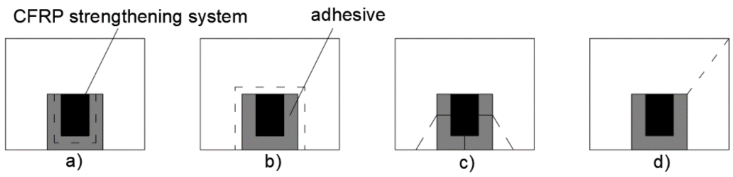

Caption:
- **mode a)**: failure at the CFRP-adhesive interface;
- **mode b)**: failure at the adhesive-concrete interface;
- **mode c)**: adhesive cover splitting;
- **mode d)**: concrete cover splitting.

Figure 2 - Failure modes by debonding of the reinforced concrete element for NSM technique (adapted of [2]).

Table 1 – Different values of the maximum design strain for EBR and NSM CFRP strengthening according to different documents (adapted of [1], [2], [3], [4], [5]).

Document	Maximum design strain of CFRP reinforcement for EBR technique	Maximum design strain of CFRP reinforcement for NSM technique
fib Bulletin 14	$\varepsilon_{f,lim} = 6.5\ a\ 8.5\ ‰$	-
fib Bulletin 90	$\varepsilon_{f,lim} = \dfrac{\beta_l \dfrac{k_{cr,k}\ k_k\ k_b \sqrt{\dfrac{2\ E_f}{t_f} f_{cm}^{2/3}}}{\gamma_{fb}}}{E_f}$	$\varepsilon_{f,lim} = \eta \dfrac{f_{fk}}{\gamma_f\ E_f}$
ACI-440.2R-17	$\varepsilon_{f,lim} = 0.41 \sqrt{\dfrac{f_c'}{E_f\ t_f}} \leq 0.9\varepsilon_{fu}$	$\varepsilon_{f,lim} = \varepsilon_{fd} = 0.7\ \varepsilon_{fu}$
CNR-DT 200 R1/2012	$\varepsilon_{f,lim} = \dfrac{\dfrac{k_q}{\gamma_{f,d}} \sqrt{\dfrac{E_f}{t_f} \dfrac{2\ k_b\ k_{G,2}}{FC} \sqrt{f_{cm}\ f_{ctm}}}}{E_f}$	-
Annex J of EC2	$\varepsilon_{f,lim} = \dfrac{\dfrac{0.17}{\gamma_{BA}}\ k_b\ \beta_1 \sqrt{\dfrac{2\ E_f}{t_f} f_{cm}^{2/3}}}{E_f}$	$\varepsilon_{f,lim} = 0.95\ b_f\ \tau_{b1d}\ \sqrt[4]{a_r}\ l_b\ (0.4 - 0.0015\ l_b)/E_f$ para $l_b \leq 115\ mm$ $\varepsilon_{f,lim} = 0.95\ b_f\ \tau_{b1d}\ \sqrt[4]{a_r}\ \left(26.2 + 0.065 \tanh\left(\frac{a_r}{70}\right)(l_b - 115)\right)/E_f$ para $l_b > 115\ mm$

Note: The variables are explained in the Appendix.

3. EBR CFRP flexural strengthening
3.1. Practical example

In order to assess the differences between the design recommendations provided in the analysed documents, this section presents a practical design example of a strengthening intervention of a building floor, where the various design methodologies are applied and the results compared. The chosen floor is part of a building that was built in 1956 with a reinforced concrete structure. As a result of a rehabilitation, the intention is to change its functionality/use from residential to a service building. In one of the floors, it is intended to install an archive area in which the overload corresponds to 6kN/m^2.

It becomes important, because of this, to define the geometry of the the slab and beam to be strengthened. In figure 3 the plan view of the slab and the location of the beam that, after structural evaluation, needs to be strengthened (beam V2) are represented. In figure 4 and figure 5, the cross sections of the beam and slab, with their respective steel reinforcement, are illustrated, respectively.

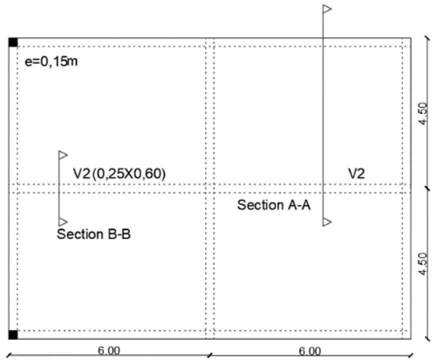

Figure 3 – Plan view of the slab.

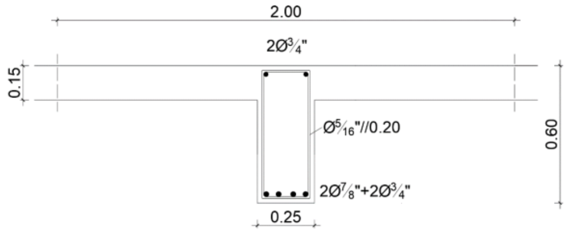

Figure 4 – Section of the beam that needs to be strengthened (Section B-B).

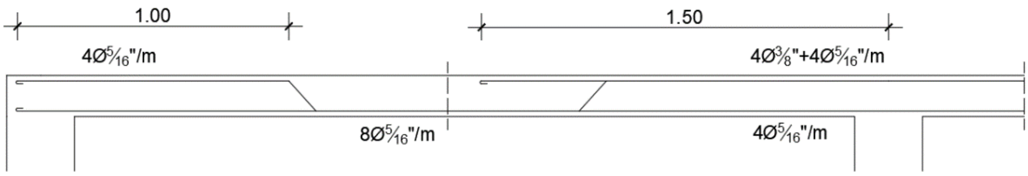

Figure 5 - Section A-A of the slab in the more stressed direction with the respective steel reinforcement.

The quantification of the actual properties of the materials of the existing structure is necessary to determine the current flexural capacity of the reinforced concrete elements. The mechanical properties of the materials needed for this assessment are shown in table 2.

Table 2 - Mechanical properties of the materials.

Mechanical properties of materials (MPa)	
E_c	30000
f_{cd}	13.30
f_{ctm}	2.20
f_{syd}	204
E_s	210000

Note: The variables are explained in the Appendix.

table 3 shows the positive bending moments capacity of the slab and the beam that are going to be strengthened (the corresponding sections are shown in figure 4 and figure 5), as well as the acting bending moments (positive) for the new use of the structure, taking advantage of a redistribution of the moments.

Table 3 – Bending moment capacity of the slab and beam V2 to be strengthened.

Case study	Positive resistant bending moment of the initial section	Acting moment after load addition (assuming redistribution of the moments)
Slab(kNm/m)	11.68	25.38
Beam (kNm)	140.70	237.45

After defining all the aspects of the critical cross sections and of their materials, the design methods to calculate the flexural strength were applied to obtain the maximum design strain for the CFRP system, as well as the necessary CFRP area.

First, the value of the maximum design strain of the CFRP system was determined, according to the different methods and recommendations of the documents, in order to determine the position of the neutral axis at the cross section and the required area of the CFRP system for the valid failure mode. In order to determine the maximum CFRP strain according to documents fib Bulletin 90, ACI, CNR and Annex J, initial values of the thickness and width of the CFRP laminate had to be assumed as a first iteration; these values were then optimized using an iterative procedure - the initial thickness and width were 1.4 mm and 120 mm, respectively.

It is important to mention that, in the calculation of the neutral axis of the section according to the different documents, it was assumed the participation steel reinforcement under compression and in a simplified way, it was taken in account a rectangular compressive distribution of the concrete. The ACI document doesn't consider the participation of the compressed steel reinforcement; however, in order to standardize the calculations, and to try to make them as comparable (and close to real) as possible, steel reinforcement under compression was taken into account. The same method was used in all the methods to get to the neutral axis position and the necessary CFRP area, these were obtained through an equation system of equilibrium of forces and assuming the bending moment shown in table 3. Afterwards, it was verified that the failure mode, for both cases, slab and beam, predicted according to all documents, was the debonding of the CFRP system.

The necessary CFRP areas to strengthen the critical sections were determined using the value of the maximum strain of CFRP system. In order to define it, it was necessary to assume from the start a modulus of elasticity for the CFRP laminate. It was decided to use one modulus of elasticity of a product sold in Portugal by the companies Sika and S&P. Taking into account that by using a higher modulus of elasticity the necessary laminate area is smaller, highest modulus of elasticity (210 GPa), which corresponds to the Type M laminate from Sika was used for both cases. However, it is worth mentioning the fact that the cost of all CFRP materials increases with their modulus of elasticity.

Table 4 presents the obtained results for the slab and the beam; from the values obtained for the maximum CFRP strain and for the resulting CFRP area needed to strengthen these elements. Looking at the values of the CFRP areas obtained, it can be understood that these are closely related to the value provided by each document for the maximum strain of the CFRP system. Since the failure mode obtained, according to the documents, for the slab and beam, was by debonding of the CFRP system, this correlation would be predictable. It can be observed that the CFRP areas have different values, according to the different approaches of the design documents in predicting the debonding strain of the CFRP system. These results show that, in practical terms, very different results can be obtained according to the document used as reference for the design of these strengthening systems.

Table 4 – Strain and area of the EBR-CFRP system obtained according to the different documents.

Case study	Document	Strain	Modulus of elasticity (MPa)	Strip design strength (MPa)	Area
Slab	*fib* Bulletin 14	0.0065	210000	910.00	0.875 cm²/m
	fib Bulletin 90	0.0017		350.44	3.703 cm²/m
	ACI-440.2R-17	0.0028		579.10	2.391 cm²/m
	CNR-DT 200 R1/2012	0.0017		367.11	2.539 cm²/m
	Annex J of EC2	0.0009		186.54	8.237 cm²/m
Beam	*fib* Bulletin 14	0.0065	210000	910.00	1.115 cm²
	fib Bulletin 90	0.0017		358.14	4.571 cm²
	ACI-440.2R-17	0.0028		579.10	2.948 cm²
	CNR-DT 200 R1/2012	0.0018		377.89	3.835 cm²
	Annex J ofEC2	0.0009		198.97	9.955 cm²

3.2. Comparison between experimental data from literature and predictions using the selected design documents

The main objective of the analysis presented in this section is to assess if the predictions for the flexural strength of RC member flexurally strengthened with CFRP systems obtained by the methods suggested in the previously mentioned documents (without safety factors), are close to actual/experimental values from tests reported in the literature. For this purpose, 3 case studies were selected, in which the geometry of the specimens (beams and slab strips), the mechanical properties of all constituent materials, including the strengthening system, were known. Two experimental beam tests and a slab strip test were chosen. It is worth mentioning that the representativeness of the results of the slab strip may have some limitation, especially due to the reduced scale/dimension of the specimens (length of 1.5 m and thickness of 0.11 m). The beams and the slab from the case studies were loaded up to failure in a 4-point bending configuration (i.e., simply supported with two point loads). It is important to mention that the mean value of the concrete compressive strength (f_{cm}) considered in the calculations for the beams were 80% of the result reported in the compression tests of cubic specimens at 28 days of age. This assumption was considered adequate because this would be the approximate compressive strength if the tests were conducted on cylindric specimens. However, for the slab strip, the average value of concrete compressive strength obtained from tests on cubic specimens at 337 days (representative age of the reinforced concrete on the day of the test on the slab) was assumed; this was due to the fact that the strip slab was heavily reinforced with steel (stirrups) imposing a significant confinement to the concrete; as a consequence, its (confined) compressive strength would be similar to that obtained from tests on cubic specimens.

Case study 1 consists in the analysis of a reinforced concrete beam, flexurally strengthened with two CFRP laminates (100x1.4 mm^2 of the type S&P Laminates CFK 200/2000) [6]. Case study 2 consists on the analysis of a reinforced concrete beam, strengthened with one CFRP laminate (80x1.4 mm^2 of the type S&P Laminates CFK 150/2000) [7]. Case study 3 comprises the analysis of a reinforced concrete slab strip strengthened with two laminates (20x1.4 mm^2 of the type S&P Laminates CFK 150/2000) [8]. table 5 shows the defining parameters and properties of the reinforced concrete, steel and laminates used in the experiments. The cross sections of the beams and slab strip of the case studies 1, 2 and 3, respectively are illustrated in figure 6, figure 7 and figure 8. For case study 1, the failure mode observed in the experimental campaign was the debonding of the laminate of CFRP, extensive cracking having occurred near the end of the laminate; for case study 2, CFRP debonding also occurred, with concrete cover splitting in the anchorage zone and, similarly, for case study 3, failure occurred due to the debonding of the CFRP laminate from the anchorage zone.

Table 5 – Steel, concrete and laminate properties for case studies 1, 2 and 3 (adapted of [6], [7], [8]).

Properties of steel reinforcement	**Case 1**	**Case 2**	**Case 3**	**Properties of concrete**	**Case 1**	**Case 2**	**Case 3**
A_{s1} (cm²)	16.10	3.02	0.85	top cover (m)	0.02	0.02	0.02
A_{s2} (cm²)	2.36	3.39	0.85	bottom cover (m)	0.02	0.04	0.02
f_{sym} (-) (MPa)	580	535	594	E_c (MPa)	30000	30000	31000
f_{sym} (+) (MPa)	580	583	594	f_{cm} (MPa)	26.97	24.80	29.50
E_s (MPa)	210000	210000	201900	f_{ctm} (MPa)	2.70	2.60	1.70
ε_{sym} (-)	0.00276	0.00255	0.00294	**Experimental results**	**Case 1**	**Case 2**	**Case 3**
Properties of CFRP laminates	**Case 1**	**Case 2**	**Case 3**	Failure load	291.7	158.9	14.95
A_f (cm²)	2.8	1.12	0.56	Strain at failure	0.0074	-	0.00315
E_f (MPa)	208000	165000	189000				
L (m)	5.6	2.5	1.1				

Note: The variables are explained in the Appendix.

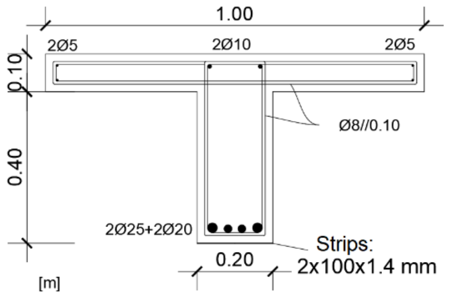

Figure 6 – Cross section of the beam in case study 1 (adapted of [6]).

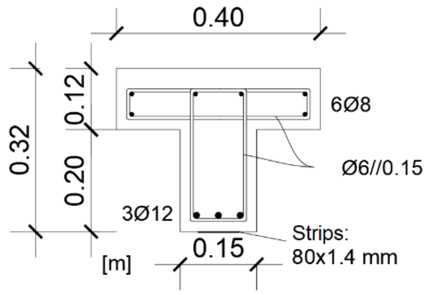

Figure 7 - Cross section of the beam in case study 2 (adapted of [7]).

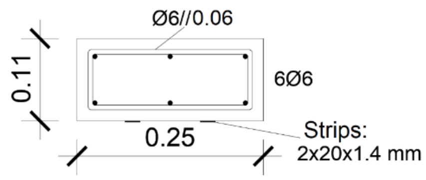

Figure 8 - Cross section of the slab strip in case study 3 (adapted of [8]).

Based on the data from the experiments presented above, the calculation methods were used to obtain the maximum strain of the CFRP system, as well as the corresponding failure load of the specimens. All calculations were carried out with safety coefficients of 1, so that the achieved results were directly comparable with the values from the experiments. Similarly, for the described process in the practical example, the value of the maximum strain of the CFRP system was determined through the various methods and recommendations in the documents. To obtain the neutral axis, the same approach was adopted for all the documents: equilibrium of forces and verification of the failure modes based of strain diagrams of the critical cross section. In this analysis, the failure mode in all cases, using all the different documents, was, also, by debonding of the CFRP laminates. Then, through the positioning of the neutral axis and with the valid failure mode, the resistant bending moment was determined based on the expressions of the various documents. With the value of the resistant bending moment, it was possible to determine the corresponding failure load for each method. Thus, table 6 shows the comparison between the predicted maximum strain of the CFRP system obtained according to the various documents and the one obtained in the tests, as well as the comparison between the experimental and predicted failure loads. It is worth mentioning that in case study 2 the strains in the CFRP were not measured during the tests.

Table 6 - Comparison between the predicted maximum strain of the EBR-CFRP system and failure loads obtained following the various documents with the experimental ones.

Case study	**Document**	**Predicted strain**	**Experimental strain**	**Predicted failure load (kN)**	**Experimental failure load (kN)**
1	*fib* Bulletin 14	0.00650	0.0074	288.41	291.7
	fib Bulletin 90	0.00542		272.91	
	ACI-440.2R-17	0.00395		259.49	
	CNR-DT 200 R1/2012	0.00415		262.24	
	Annex J of EC2	0.00176		136.47	
2	*fib* Bulletin 14	0.00650	-	80.07	79.45
	fib Bulletin 90	0.00552		74.23	
	ACI-440.2R-17	0.00425		69.10	
	CNR-DT 200 R1/2012	0.00409		76.45	
	Annex J of EC2	0.00179		32.48	
3	*fib* Bulletin 14	0.00650	0.00315	22.99	14.95
	fib Bulletin 90	0.00595		21.69	
	ACI-440.2R-17	0.00433		18.53	
	CNR-DT 200 R1/2012	0.00367		18.25	
	Annex J of EC2	0.00193		8.33	

First, it is necessary to understand that the analysis of results must be done separately for the slab strip; as previously mentioned, its representativeness is limited because of its reduced scale. Thus, the results obtained for the beams are the next to be analysed (case studies 1 and 2).

By looking at the results predicted for the beams and comparing them with the values obtained on the experimental campaigns, it can be seen that they are very conservative.

Regarding *fib* Bulletin 14, it recommends a fixed value for the maximum CFRP strain and doesn't clarify if this value is affected by safety coefficients. Thus, a decision was made to assume an average value, however, this could be higher and even if it is affected by safety factor, it is the closest value to the experimental ones.

The value of the maximum CFRP strain of the remaining documents was obtained through the different formulas presented in table 1, based on the characteristics of the CFRP system and of the reinforced concrete previously shown. One of the possible explanations for the predicted values being inferior to the experimental ones could be the reinforced concrete properties, specifically the mean value of concrete compressive and tensile strength, because they are referred to tests conducted at 28 days of age. It is known, however, that the experimental tests on the beams were performed at a date later than 28 days, therefore the mean values of the concrete compressive and tensile strengths at the time of the tests could have been higher than the figures used in the calculations; with higher values of the concrete properties, the maximum CFRP strain values would also be higher.

It is important to mention that the formulas proposed in the documents include some empirical factors/constants that were experimentally calibrated and are very conservative; in fact, they are the conditioning factor of the values for the maximum CFRP strain. As an example of this, the $k_{G,2}$ factor, present in the formula in table 1 from the CNR document, that suggests a value of 0.2 mm, has a significant influence on the maximum strain. This, consequently, results in a maximum predicted strain that is significantly lower than the one achieved in the corresponding experimental campaign.

Regarding the values obtained for the slab strip, only the strain from Annex J is inferior to the one obtained in the tests. However, it has to be noticed, the maximum CFRP strain measured in this test was relatively low and only one test was performed (with no repetitions). This type of tests, and in particular the debonding phenomenon of the CFRP strengthening systems, exhibit a high intrinsic variability, making this result less reliable. Another important aspect, as previously mentioned, is the reduced scale of this slab, leaving doubts about its representativeness. However, the relative differences between the results predicted according to the various documents, are similar to the ones achieved on the beam tests. The analysis of an element with smaller dimensions allowed to conclude that the fact that *fib* Bulletin 14 recommends a fixed value for the maximum CFRP strain may not be adequate, as the material properties and the geometry of the elements and their internal steel reinforcement may affect the mechanical performance of the CFRP system.

When it comes to Annex J, it presents two different methods to get the maximum CFRP strain, one simple method and more complex one. Although it was not expected, when using the more complex method, the value of the CFRP strain achieved was lower than the one obtained using the simplified method. This may be partially explained by the fact that the more complex method includes some corrective factors that, even though calibrated based on the experiments, are very conservative, originating a lower strain when compared to the one from the case studies. In this context, it was decided to use the values from the simplified method to estimate the failure load because these were closer to the ones achieved in the experiments.

Regarding the results predicted for the failure load, since the failure mode obtained according to all the documents was CFRP debonding, the calculation of the neutral axis and of the resistant bending moment were based on the value of the maximum strain of the CFRP system. As such, the value of the maximum strain given by each document the main conditioning factor for the final value of the failure load. This means that the higher the maximum strain is (and closer to the experimental value), the higher the failure load will be, and, therefore, the closer to the experimental value. As such, it can be concluded that the best prediction of the experimental values for the tests on beams was achieved by the calculating methods of *fib* Bulletin 14 and the worst from Annex J.

On the other hand, the fact that the values adopted in the calculations for the concrete compressive and tensile strengths (at 28 days) were lower than the actual concrete properties of the beams may explain (at least partially) the difference between the predicted and experimental failure loads.

Regarding the slab strip, the obtained results for the failure load are coherent with the analyses done on the maximum strain of CFRP system. Once again, only the value from Annex J is significantly inferior to the experimental one. Given that the failure mode achieved, similarly to the beams, was CFRP debonding, the strain values achieved are the main conditioning factor and, as such, the results are the expected ones.

4. NSM CFRP flexural strengthening

4.1. Practical example

Similarly to what was done in the previous section for the EBR system a NSM-CFRP system was designed to strengthen the same building floor. The residence building in consideration was already presented in section 3.1. The main goal of this analysis is to design the necessary reinforcement areas accordingly to the various methodologies proposed in the different documents and to compare the differences between them and the two strengthening techniques (EBR *vs*. NSM).

The calculation methods for the design of the NSM strengthening system were applied in order to get the maximum CFRP strain (cf. table 1) as well as the necessary laminate area for the CFRP system. Overall, the calculation methods are similar to those used for the EBR system, the main difference being the calculation of the maximum CFRP strain of the NSM system. According to the *fib* Bulletin 90 and ACI documents, in order to determine the maximum CFRP strain it is necessary from the start to define the tensile strength and the laminate modulus of elasticity, as such, these values were initially assumed based on properties of commercially available products from S&P and Sika. The considered values are shown in table 7. According to the Annex J document from EC2, it was not only necessary to assume the value of the modulus of elasticity, but also each laminate area; for the effect an area of 0.28 cm^2 was initially assumed (laminates with a width of 20 mm and a thickness of 1.4 mm).

As assumed in the calculations of the area of the EBR system, in the calculation of the neutral axis of the cross section according to the different documents, the participation of the compressive steel reinforcement was considered, and, as simplification, a rectangular compressive stress block was assumed for the concrete.

To get to the neutral axis and the necessary laminate area a similar approach to the one presented for the EBR system was adopted (with the natural differences of the geometry and the maximum strain of the NSM system). The obtained CFRP areas correspond to the resistant bending moment shown in table 3 (25.38 kNm/m for the slab and 237.50 kNm for the beam).

The results obtained for the slab and beam are presented in table 7.

Table 7 - Strain and area of the NSM-CFRP system obtain for all the different documents.

Case study	Document	Strain	Modulus of elasticity (MPa)	Strip design strength (MPa)	Area
Slab	*fib* Bulletin 90	0.0109	168000	2850	0.695 cm²/m
	ACI-440.2R-17	0.0119			0.832 cm²/m
	Annex J of EC2	0.0064			1.148 cm²/m
Beam	*fib* Bulletin 90	0.0109	168000	2850	0.823 cm²
	ACI-440.2R-17	0.0119			0.889 cm²
	Annex J of EC2	0.0063			1.435 cm²

By observing the values obtained for the NSM laminate areas, it is possible to draw conclusions resembling those obtained for the EBR system; it can be understood that these are directly related to the predicted value for each document for the maximum strain of the CFRP system. Given that the failure mode achieved according to all the documents for the slab and beam was CFRP debonding, this dependency was expected.

The conclusions obtained from the analysis of the achieved results are similar to those of the EBR system - once again, the CFRP areas present different values depending on the approaches adopted by the documents to predict the maximum CFRP strain. Therefore, it becomes important to compare the results achieved according to the different documents with the ones obtained in experimental tests reported in the literature, so that it becomes possible to assess with more detail the level of precision of the different methodologies in predicting the actual/real flexural strength of reinforced concrete structures strengthened with CFRP systems, installed accordingly to the NSM technique.

4.2. Comparison between experimental data from literature and predictions using the selected design documents

Similarly to tests described in section 3.2 for the EBR system, the beams and the slab strengthened with the NSM-CFRP laminates were also tested up to failure using a 4-point bending configuration. Regarding the mean values of concrete compressive strengths (f_{cm}) used in the beams, these were obtained by means of compressive tests in cylindrical specimens at the time of the experiments in the beams. In the case study about the slab strip, it is the same as the one presented in the EBR system section, the only difference being the type of strengthening system. Case study 1 consists in the analyses of a reinforced concrete beam strengthened with two laminates (section 10x1.4 mm^2 of the type S&P Laminates CFK 150/2000) [9]; case study number 2 consists in the analyses of a reinforced concrete beam strengthened with four laminates (section 15x1.4 mm^2 of the type S&P Laminates CFK 150/2000) [10] and case study 3 consists in the analyses of a reinforced concrete slab strip strengthened with two laminates (section 10x1.4mm^2 of the type S&P Laminates CFK 150/2000) [8]. The necessary characteristics to define the reinforced concrete, steel and laminates used in the experiments are presented in table 8. The cross section of the beams and slab strip of each case study are shown in figure 9, figure 10 and figure 11. For case study 1 the failure mode of the beam was by debonding of the CFRP system in the anchorage zone. In case study 2, the failure mode was by pealing-off of the concrete cover including the CFRP system. Finally, in case study 3, the failure mode was by debonding of the CFRP system caused by shear cracks.

Table 8 - Steel, concrete and laminate properties for case study 1, 2 and 3 (adapted of [9], [10], [8]).

Properties of steel reinforcement	**Case 1**	**Case 2**	**Properties of concrete**	**Case 1**	**Case 2**	**Properties of CFRP laminates**	**Case 1**	**Case 2**	**Case 3**
A_{s1} (cm²)	1.57	2.356	top cover (m)	0.02	0.02	A_f (cm²)	0.28	0.846	0.28
A_{s2} (cm²)	1.01	2.356	bottom cover (m)	0.02	0.02	E_f (MPa)	175000	158000	168000
f_{sym} (-) (MPa)	534.5	465.75	E_c (MPa)	30000	31170	L (m)	2.3	1.4	1.1
f_{sym} (+) (MPa)	534.5	465.75	f_{cm} (MPa)	50.2	53.1	**Experimental results**	**Case 1**	**Case 2**	**Case 3**
E_s (MPa)	210000	200318	f_{ctm} (MPa)	4.08	4.24	Failure load	55.95	73.65	22.9
ε_{sym} (-)	0.00255	0.00233				Strain at failure	0.0174	0.00976	0.0116

Note: The variables are explained in the section Appendix.

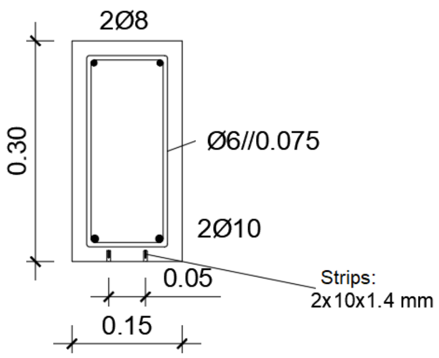

Figure 9 - Cross section of the beam in case study 1 (adapted of [9]).

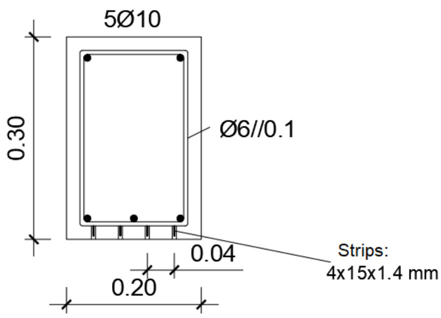

Figure 10 - Cross section of the beam in case study 2 (adapted of [10]).

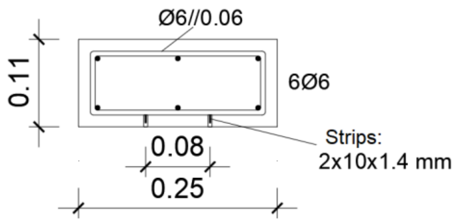

Figure 11 - Cross section of the slab strip in case study 3 (adapted of [8]).

Similarly to what was done for the EBR system, the calculation methods were used to predict the maximum strain of the CFRP system as well as the failure load of the specimens. All calculations were done considering unitary safety coefficients, so that the results achieved would be the closest to actual/real behaviour observed in the experimental campaigns.

As in the process described for the EBR system in section 3.2, the value of the maximum strain of the CFRP system was determined according to the different methods and recommendations of the documents. Calculation methods are similar for both systems, the main difference being the proposals for the maximum CFRP strain.

Table 9 shows the comparison between the predictions for the maximum CFRP strain and the failure loads of the specimens obtained according to the various documents with the corresponding experimental values.

Table 9 - Comparison between the predicted maximum strain of the NSM-CFRP system and failure loads obtained according to the various documents with the experimental ones.

Case study	**Document**	**Predicted strain**	**Experimental strain**	**Predicted failure load (kN)**	**Experimental failure load (kN)**
1	*fib* Bulletin 90	0.01447	0.0174	45.82	55.95
	ACI-440.2R-17	0.01266		43.44	
	Annex J of EC2	0.00545		31.89	
2	*fib* Bulletin 90	0.01233	0.00976	80.86	73.65
	ACI-440.2R-17	0.01079		75.43	
	Annex J of EC2	0.00656		57.88	
3	*fib* Bulletin 90	0.01357	0.0116	20.46	22.9
	ACI-440.2R-17	0.01188		19.30	
	Annex J of EC2	0.00668		14.50	

By analysing the predicted CFRP strains, it can be noticed that the results obtained according to documents *fib* Bulletin 90 and ACI for case studies 2 and 3 are higher than the experimental but inferior to those obtained according to document Annex J. On the other hand, for case study 1 the predicted maximum strains are lower than the experimental ones. Regarding to the calculation method of the maximum CFRP strain, documents *fib* Bulletin 90 and ACI present a very similar approach, but with different safety coefficients. Document *fib* Bulletin 90 multiplies the CFRP failure strain by 0.8, whereas in ACI it is by 0.7. The calculation method recommended by Annex J from EC2 is more complex and includes different variables related to the type of reinforced concrete and the type of adhesives used. Regarding the adhesive, this formula takes into account its mean values of compressive and tensile strengths. In the case studies, all of them used the same type of adhesive, Resin 220 by S&P, that, according to the manufacturer, presents values for the compressive and tensile strength of 30 MPa and 90 MPa, respectively. As consequence, the values obtained for the maximum CFRP strain using this document are the most conservative ones.

Concerning the predicted values of the failure load, as in the EBR technique, and since the failure mode predicted according to all documents was by debonding of the CFRP laminate, the calculations for the neutral axis and for the resistant bending moment were made based on maximum CFRP strain. Therefore, the value of the maximum strain given by each document the main conditioning factor for the predicted failure loads. This means that, the higher the value of the maximum CFRP strain is, the higher will be the corresponding failure load, and, for case studies 1 and 2, the closer to experimental values. However, this was not verified for case study 3, because even though the maximum strains for documents *fib* Bulletin 90 and ACI are higher than the strain measured in the experimental campaign, the failure loads determined according to the documents are lower than the experimental one. It is worth remembering the fact that the slab is of reduced scale, and therefore the representativeness of conclusion derived from this analysis may be limited.

Overall, it can be concluded that the document adopted for design of the strengthening system has a significant influence on the result in terms of CFRP area needed.

5. Conclusion

The main goal of this dissertation was to analyse and compare the methodologies proposed on the main international documents for the design of reinforced concrete structures flexurally strengthened with CFRP systems, enabling an assessment of the impact (in terms of area of CFRP material needed) of the methodology adopted.

The literature review allowed to analyze the recommendations made for the design of CFRP strengthening systems, either applied according to externally bonded reinforcement (EBR) technique or the near surface mounted (NSM) one. It was possible to find the common and divergent aspects between the different philosophies for the design of these CFRP systems. From this assessment, it was understood that the biggest divergency in the design recommendations was about the design CFRP strain (associated with the phenomenon of the debonding of the CFRP system). This aspect has the biggest influence in the necessary strengthening area of CFRP system, because the most common/conditioning failure mode is by debonding of CFRP system, which limits the maximum CFRP strain that can be mobilized.

In order to make it possible to compare the calculation methods presented in the analysed documents, for the flexural safety verification of the reinforced concrete slabs and beams strengthened with CFRP systems applied using the EBR and NSM techniques, automatic calculation sheets were developed, where the different design methodologies were implanted. Using this calculating tool, the flexural strengthening systems (for both EBR and NSM techniques) were designed for a slab and beam of a practical example; then a comparative study was performed, using experimental results reported in the literature and the predictions for the maximum CFRP strain and the corresponding failure loads of the specimens obtained using the proposed methodologies by the various documents.

When observing the results from the practical example for both EBR and NSM systems, the values obtained for the areas of CFRP system are directly related with the values of the maximum strain of the CFRP system. This relation was expected since the failure mode obtained for all documents for the slab and beam was by debonding of the CFRP system. The obtained CFRP areas have significantly different values depending on the documents adopted to predict the maximum CFRP strain (associated to the debonding). These results show that in practical design situations, very different strengthening solutions can be obtained depending on the document adopted for the design of these systems.

Regarding the comparison between the experimental values and the ones predicted by the different documents, it was concluded that the predicted values of both the maximum CFRP strain and failure load are, overall, very conservative, i.e., lower than the experimental ones for both strengthening techniques.

With the development of the present dissertation, it was possible to conclude that, in general, the values suggested by the documents for the maximum strain of the CFRP system substantially limit the capacity of this type of strengthening to increase the flexural capacity of these structural elements; as a consequence, only a fraction of the actual flexural strength capacity of the strengthening system is explored. Regarding the upcoming version of the Eurocode 2 (EC2) that will include an informative annex (J) about the design of CFRP strengthening systems, it was concluded that the approaches adopted in this document, both for EBR and NSM systems, are significantly more conservative than the ones recommended by the other documents, leading to overdesigned and uneconomical strengthening solutions.

References

[1] Fib bulletin 14, “Externally bonded FRP reinforcement for RC structures”, Fédération Internacionale du Béton (fib), Task Group 9.3 FRP, Lausanne, 2001.

[2] Fib bulletin 90, “Externally applied FRP reinforcement for concrete structures”, Fédération Internacionale du Béton (fib), Task Group 5.1 FRP, Lausanne, 2019.

[3] ACI 440.2R-17, “Guide for the Design and Construction of Externally Bonded FRP Systems for Strengthening Concrete Structures”, American Concrete Institute, 2017.

[4] CNR-DT 200 R1/2013, “Guide for the Design and Construction of Externally Bonded FRP Systems for Strengthening Existing Structures”, CNR – Advisory Committee on Technical Recommendations for Construction, 2014.

[5] EN 1992-1-1:2020 (E), “Annex J Strengthening of Existing Concrete Structures with CFRP”.

[6] P. França, A. Costa, & J. Appleton, “Evaluation of the Performance of Anchoring Systems for the External Flexural Strengthening of RC Beams”, Instituto Superior Técnico, 2003.

[7] Duarte, P., “Estudo experimental do efeito da reparação de fendas no comportamento de vigas de betão armado reforçadas à flexão com laminados de CFRP”, Instituto Superior Técnico, 2011.

[8] Azevedo, A., Firmo, J., Correia, J., Chastre, C., Biscaia, H., Franco, N., “Composites Part B -Fire behaviour of CFRP-strengthened RC slabs using different techniques – EBR, NSM and CREatE”, Paper, Instituto Superior Técnico, Maio 2021.

[9] Dias, S., Barros, J., Azevedo, C., “Comportamento de vigas de betão armado reforçadas à flexão com laminados de CFRP inseridos”, master dissertation, FEUP, outubro 2012.

[10] Coelho, M., Silva, L., Sena-Cruz, J.M., Barros, J., “Estudo comparativo de diferentes técnicas no reforço à flexão de vigas de betão armado com recurso a CFRP’s sob acções monotónicas e de fadiga.” Revista Portuguesa de Engenharia de Estruturas, 2011.

Appendix

A_f	Area of CFRP reinforcement
A_{s1}	Area of steel reinforcement subjected to tension
A_{s2}	Area of steel reinforcement subjected to compression
a_r	Distance from the longitudinal axis of the CFRP system to the free edge (page 21 of the dissertation)
b_f	Width of CFRP reinforcement
E_c	Modulus of elasticity of concrete
E_f	Modulus of elasticity of CFRP reinforcement
E_s	Modulus of elasticity of steel reinforcement
FC	Confidence factor (page 26 of the dissertation)
$f_c{}'$	Mean value of concrete compressive strength
f_{cd}	Design concrete compressive strength
f_{cm}	Mean value of concrete compressive strength
f_{ctm}	Mean value of concrete tensile strength
f_{fk}	characteristic strength of CFRP reinforcement
f_{syd}	Design yield strength of longitudinal steel reinforcement
f_{sym}	Mean yield strength of longitudinal steel reinforcement
k	Page 17 of the dissertation
k_b	Factor that takes into account the bond geometry (page 19 of the dissertation)
k_{cr}	Page 17 of the dissertation
$k_{G,2}$	Corrective factor (page 26 of the thesis)
k_q	Coefficient that takes into account the load distribution (page 26 of the dissertation)
L	Element length
l_b	Bond length
t_f	Thickness of CFRP laminate
β_1	Factor that depends on the bond length (page 19 of the dissertation)
β_l	Factor that depends on the bond length (page 19 of the dissertation)
γ_{BA}	Safety coefficient of permanent/transient bonding material (page 29 of the dissertation)
γ_f	Safety coefficient of CFRP strength material (page 18 of the dissertation)
γ_{fb}	Safety coefficient of permanent/transient bonding material (page 17 of the dissertation)
$\gamma_{f,d}$	Partial factor of CFRP materials (page 26 of the dissertation)
ε_{fd}	Maximum value for the design strain of CFRP system
ε_{fu}	Maximum strain of CFRP system
ε_{sym}	Yield strain of steel reinforcement
η	Limit coefficient for tensile strength of the FRP (page 18 of the dissertation)
τ_{b1d}	Bond resistance (page 21 of the dissertation)